(Preprint) AAS 22-732

RECONSTRUCTION OF PARTICLE DISPERSION EVENTS WITH OPTICAL MEASUREMENTS

Anonto Zaman* and John A. Christian†

Discrete particle ejection events are known to periodically occur on the asteroid Bennu. Similar phenomena may also occur on other small bodies in our Solar System. If these particle events are observed by the camera aboard an exploration spacecraft, as was the case with the OSIRIS-REx spacecraft during its visit to Bennu, then the apparent motion of particles may be used to reconstruct the event. This work explores the utility of algebraic projective geometry for performing this reconstruction and the resulting algorithms are shown to have many practical advantages when compared to earlier methods. The algorithms are further tested through numerical simulation, including cases with varying numbers of particle observations.

INTRODUCTION

The OSIRIS-REx mission to asteroid Bennu [1] serendipitously witnessed a number of discrete particle ejection events on the asteroid's surface [2]. These unexpected events occur through a natural process, where particles of diameters < 10 cm are energetically expelled from a point on the body's surface. If the individual ejected particles can be observed and tracked from a spacecraft camera, it is possible to reconstruct their trajectories and determine the point of origin on the asteroid surface [3]. It is reasonable to conjecture that such events may occur on other small bodies within our solar system—thus, techniques to model such events are important for future missions.

In this work, we seek to deploy concepts from algebraic projective geometry [4] to enhance our ability to interpret particle dispersion events observed by a spacecraft camera. This same mathematical framework has recently yielded impressive results for horizon-based optical navigation (OPNAV) [5], lunar crater identification [6], star pattern identification [7], and absolute triangulation [8]. An introductory tutorial aimed at the spacecraft navigator may be found in Ref. [5] and some of the foundational theory may be found in Ref. [4]. As compared to the method developed for OSIRIS-REx in Ref. [3], the approach shown here results in a simpler algorithm and enhanced geometric insight. We note that the procedure discussed here bears many similarities to the concept of "dynamic triangulation" recently introduced by Henry and Christian [8].

GEOMETRY OF LINEAR PARTICLE EVENTS

Suppose a particle event occurs at an unknown time t_0 and produces n particles. Let the location of this event in an inertial frame be $\boldsymbol{p}_0 \in \mathbb{R}^3$, such that all particles are located at $\boldsymbol{p}_0$ at time t_0. Note that neither $\boldsymbol{p}_0$ nor t_0 are known beforehand. Now, suppose that the kth particle departs $\boldsymbol{p}_0$ with a constant velocity $\boldsymbol{w}^{(k)}$ such that the particle position at some time $t_i > t_0$ is given by

$$\boldsymbol{p}_i^{(k)} = (t_i - t_0)\boldsymbol{w}^{(k)} + \boldsymbol{p}_0 \tag{1}$$

Like $\boldsymbol{p}_0$ and t_0, the all of the particle velocities $\{\boldsymbol{w}^{(k)}\}_{k=1}^n$ are unknown beforehand. A constant velocity is a reasonable assumption for energetic trajectories over short time intervals for many small bodies with low gravity.

*Undergraduate Student, Guggenheim School of Aerospace Engineering, Georgia Institute of Technology, Atlanta, GA 30332.
†Associate Professor, Guggenheim School of Aerospace Engineering, Georgia Institute of Technology, Atlanta, GA 30332.

Now, consider a spacecraft traveling at a constant velocity $\boldsymbol{v}$ that observes this particle event with a camera. It follows, then, that the position of the spacecraft at time t_i is given by

$$\boldsymbol{r}_i = (t_i - t_0)\boldsymbol{v} + \boldsymbol{r}_0 \tag{2}$$

We assume that the spacecraft position and velocity are known. However, since we do not know t_0 beforehand, we cannot retrieve the position $\boldsymbol{r}_0$ until we first solve for the event time t_0.

If a particle appears as a point in an image, then the corresponding image-derived measurement is a simply bearing measurement. We assume that this bearing is known in a specified inertial frame (e.g., ICRF) since we determine the camera attitude using stars in each image [7]. Thus, a camera produces an inertial bearing measurement to each particle at each measurement time. The bearing measurement simply describes a direction (it is a point in $\mathbb{P}^2$), which lies along the line connecting the camera and particle. The vector from the camera to the particle is given by

$$\boldsymbol{p}_i^{(k)} - \boldsymbol{r}_i = (t_i - t_0)\left(\boldsymbol{w}^{(k)} - \boldsymbol{v}\right) + (\boldsymbol{p}_0 - \boldsymbol{r}_o) \tag{3}$$

Letting $\boldsymbol{b}_i^{(k)} = \boldsymbol{p}_i^{(k)} - \boldsymbol{r}_i$ be the particle's camera-relative position and $\boldsymbol{a}^{(k)} = \boldsymbol{w}^{(k)} - \boldsymbol{v}$ be the the particle's camera-relative velocity, this is simply

$$\boldsymbol{b}_i^{(k)} = (t_i - t_0)\boldsymbol{a}^{(k)} + \boldsymbol{b}_0 \tag{4}$$

such that the direction of the bearing measurement we seek is

$$\boldsymbol{\ell}_i^{(k)} \propto (t_i - t_0)\boldsymbol{a}^{(k)} + \boldsymbol{b}_0 \tag{5}$$

where $\boldsymbol{\ell}_i^{(k)}$ has arbitrary scale since $\boldsymbol{\ell}_i^{(k)} \in \mathbb{P}^2$. We observe here that $\boldsymbol{a}^{(k)}$ is constant since both camera and particle have constant inertial velocities and that $\boldsymbol{b}_0$ is the camera-relative position of the particle event. The geometry of the camera relative motion is shown in Fig. 1.

PROCEDURE FOR EVENT RECONSTRUCTION WITH ONLY BEARING MEASUREMENTS

Assume the geometry from the prior section, it is possible to reconstruct the event to an unknown scale using only bearing measurements. The scale ambiguity may be removed if a reasonable 3D model of the observed body is available. The procedure consists of three separable steps: first compute the event camera-relative direction $\boldsymbol{\ell}_0 \propto \boldsymbol{b}_0$, second compute the event time t_0, third compute the camera-relative velocity of each particle $\boldsymbol{a}^{(k)}$.

Finding Direction to Particle Event

We begin with finding the camera-relative direction to the particle event. This can be achieved by observing (at least) two particles in two images.

Consider the bearings to the kth particle at times t_i and t_j. Taking the cross-product of these bearings and substituting from Eq. (5) yields

$$\boldsymbol{\ell}_i^{(k)} \times \boldsymbol{\ell}_j^{(k)} \propto (t_i - t_j)\left(\boldsymbol{a}^{(k)} \times \boldsymbol{b}_0\right) \tag{6}$$

From the right-hand side, we see that this cross-product must be orthogonal to $\boldsymbol{b}_0$, thus

$$\left(\boldsymbol{\ell}_i^{(k)} \times \boldsymbol{\ell}_j^{(k)}\right)^T \boldsymbol{b}_0 = 0 \tag{7}$$

We see here that any vector in the direction of $\boldsymbol{b}_0$ also satisfies this equation. Hence, let $\boldsymbol{\ell}_0 \in \mathbb{P}^2$ be defined as the direction $\boldsymbol{\ell}_0 \propto \boldsymbol{b}_0$ and

$$\left(\boldsymbol{\ell}_i^{(k)} \times \boldsymbol{\ell}_j^{(k)}\right)^T \boldsymbol{\ell}_0 = 0 \tag{8}$$

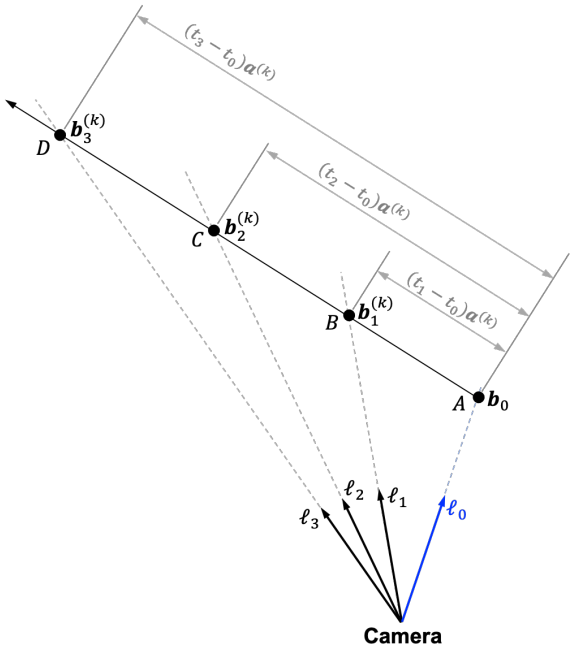

Figure 1. Illustration of camera-relative particle trajectory, with three bearing measurements to the particle shown in black ($\boldsymbol{\ell}_1, \boldsymbol{\ell}_2, \boldsymbol{\ell}_3$). The particle emanates from camera-relative location $\boldsymbol{b}_0$ with a constant camera-relative velocity $\boldsymbol{a}^{(k)}$. The time of the particle event t_0 and the bearing $\boldsymbol{\ell}_0$ are not known a priori.

where $\boldsymbol{\ell}_0$ has arbitrary scale.

If we have $n \geq 2$ images, we may stack Eq. (8) into the linear system

$$\begin{bmatrix} \left(\boldsymbol{\ell}_1^{(1)} \times \boldsymbol{\ell}_2^{(1)}\right)^T \\ \vdots \\ \left(\boldsymbol{\ell}_1^{(n)} \times \boldsymbol{\ell}_2^{(n)}\right)^T \end{bmatrix} \boldsymbol{\ell}_0 = \mathbf{0}_{n \times 1} \tag{9}$$

This is a standard null space problem, and we find the optimal value of $\boldsymbol{\ell}_0$ in the least-squares sense by using the singular value decomposition (SVD).

Finding Time of Particle Event (Three Observations)

We may obtain a linear equation for the event time t_0 directly from the cross-ratio. The cross-ratio—one of the most fundamental concepts from algebraic projective geometry [4]—is defined as

$$Cr(A, B; C, D) = \frac{AC}{CB} \Big/ \frac{AD}{DB} = \frac{A'C'}{C'B'} \Big/ \frac{A'D'}{D'B'} = \frac{\sin AVC}{\sin CVB} \Big/ \frac{\sin AVD}{\sin DVB} \tag{10}$$

where A, B, C, D are four collinear points as described in Fig. 2.

To make things simple, we also labeled the particle points with A, B, C, D in Fig. 1. Thus, we immediately recognize this particle event problem as a cross-ratio problem. We may compute the cross-ratio c along the particle's path

$$c = \frac{a^{(k)}(t_2 - t_0)\, a^{(k)}(t_3 - t_1)}{a^{(k)}(t_2 - t_1)\, a^{(k)}(t_3 - t_0)} = \frac{(t_2 - t_0)(t_3 - t_1)}{(t_2 - t_1)(t_3 - t_0)} \tag{11}$$

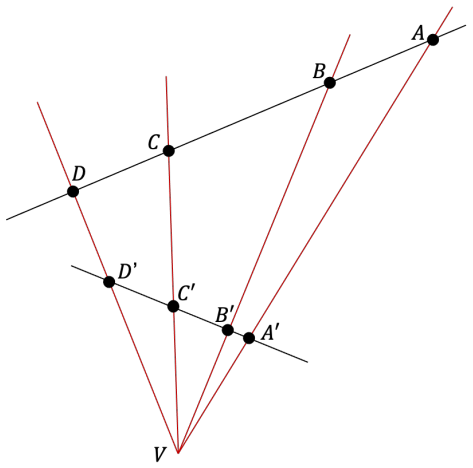

Figure 2. Illustration of cross-ratio.

which is linear in the unknown t_0. Likewise, we may compute the cross-ratio c using the angles

$$c = \frac{\|\boldsymbol{\ell}_0 \times \boldsymbol{\ell}_2\| \, \|\boldsymbol{\ell}_1 \times \boldsymbol{\ell}_3\|}{\|\boldsymbol{\ell}_1 \times \boldsymbol{\ell}_2\| \, \|\boldsymbol{\ell}_0 \times \boldsymbol{\ell}_3\|} \tag{12}$$

where we have made use of the cross-product identity $\|\boldsymbol{\ell}_1 \times \boldsymbol{\ell}_2\| = \ell_1 \ell_2 \, \sin\theta_{12}$.

Now, since Eq. (11) is linear in the unknown t_0, we may rearrange to find

$$t_0 = \frac{t_2(t_3 - t_1) - c\, t_3(t_2 - t_1)}{(t_3 - t_1) - c(t_2 - t_1)} \tag{13}$$

where we compute c directly from the bearing measurements using Eq. (12).

Finding Particle Velocity

Once the event time t_0 is known, it is possible to solve for each particle velocity up to an unknown scale. To see, this, take the cross product of Eq. (5) with the bearing,

$$(t_i - t_0) \left[\boldsymbol{\ell}_i^{(k)} \times\right] \boldsymbol{a}^{(k)} + b_0 \left[\boldsymbol{\ell}_i^{(k)} \times\right] \boldsymbol{\ell}_0 = \mathbf{0}_{3\times 1} \tag{14}$$

where $b_0 = \|\boldsymbol{b}_0\|$. If there are $n \geq 2$ observations, then

$$\begin{bmatrix} (t_1 - t_0) \left[\boldsymbol{\ell}_1^{(k)} \times\right] & \left(\boldsymbol{\ell}_1^{(k)} \times \boldsymbol{\ell}_0\right) \\ \vdots & \vdots \\ (t_n - t_0) \left[\boldsymbol{\ell}_n^{(k)} \times\right] & \left(\boldsymbol{\ell}_n^{(k)} \times \boldsymbol{\ell}_0\right) \end{bmatrix} \begin{bmatrix} \boldsymbol{a}^{(k)} \\ b_0 \end{bmatrix} = \mathbf{0}_{3n\times 1} \tag{15}$$

and we can $\boldsymbol{a}^{(k)}$ and b_0 in the least squares sense using the SVD. Since the right-hand side is zero, $\boldsymbol{a}^{(k)}$ and b_0 may only be found up to an unknown scale.

To remove the unknown scale, we can cast a ray along the direction $\boldsymbol{\ell}_0$ at time t_0 to see where it intersects the body. In general, there will be two intersection points—one closer to the camera where the ray intersects the body and one farther away from the camera where the ray exits the body on the other side. The closer intersection point is the only one that would be visible at t_0, as any other intersection points are occulded by the body. The correct intersection point may usually be disambiguated by ensuring the particle velocity doesn't pass through the body.

Finding More Particles

Once we've found at least one particle track, we may compute the cross-ratio from Eq. (12). We also observe from Eq. (11) that the cross-ratio for a particle with constant velocity is only a function of the observation times. Hence we can look at any set of three observations that are (nearly) collinear with $\boldsymbol{\ell}_0$ and immediately determine if they could have come from the same particle event by checking their cross-ratio. This may allow us to quickly find more candidate particles in an automated way.

THE SPECIAL CASE OF ONLY TWO OBSERVATIONS

It is impossible to solve for the event time and location with only two observations of each particle under the assumed (linear) dynamics. However, it is possible to limit the range of possible event times and the corresponding locus of possible event locations. This may be done my intersecting the reference direction $\boldsymbol{\ell}_0$ with the body at a range of plausible times. When the observed body is modeled as a triaxial ellipsoid, finding the intersection points at any hypothesized event time is analytic.

Consider a body modeled as a triaxial ellipsoid with principal axis lengths $\{a, b, c\}$. The body's shape matrix in the principal axis frame is

$$\boldsymbol{A}_P = \begin{bmatrix} 1/a^2 & 0 & 0 \\ 0 & 1/b^2 & 0 \\ 0 & 0 & 1/c^2 \end{bmatrix} \tag{16}$$

Now, if $\boldsymbol{T}_P^{C_k}$ is describes the rotation from the inertial frame to spacecraft camera frame at time t_k to the body's principal axis frame, then

$$\boldsymbol{A}_{C_k} = \boldsymbol{T}_{C_k}^{P} \boldsymbol{A}_P \boldsymbol{T}_P^{C_k} \tag{17}$$

If the camera-relative center of the body is given by $\boldsymbol{b}_c$, then a point $\boldsymbol{b}$ lies on the ellipsoidal bodies surface when

$$(\boldsymbol{b} - \boldsymbol{b}_c)^T \boldsymbol{A}_{C_k} (\boldsymbol{b} - \boldsymbol{b}_c) = 1 \tag{18}$$

Since the point $\boldsymbol{b}_0 = b_0 \boldsymbol{\ell}_0$ lies on the surface,

$$(b_0 \boldsymbol{\ell}_0 - \boldsymbol{b}_c)^T \boldsymbol{A}_{C_k} (b_0 \boldsymbol{\ell}_0 - \boldsymbol{b}_c) = 1 \tag{19}$$

which is quadratic in the unknown b_0. This results in the scalar quadratic equation

$$\left(\boldsymbol{\ell}_0^T \boldsymbol{A}_{C_k} \boldsymbol{\ell}_0\right) b_0^2 - 2\left(\boldsymbol{b}_c^T \boldsymbol{A}_{C_k} \boldsymbol{\ell}_0\right) b_0 + \left(\boldsymbol{b}_c^T \boldsymbol{A}_{C_k} \boldsymbol{\ell}_c - 1\right) = 0 \tag{20}$$

which may be solved analytically for b_0. If the direction $\boldsymbol{\ell}_0$ intersects the body then there will be two positive real roots, describing the two points where the ray pierces the ellipsoid. If the direction $\boldsymbol{\ell}_0$ is tangent to the body, it describes a horizon point and then there are a pair of repeated, positive, real roots. If the direction $\boldsymbol{\ell}_0$ does not intersect the body, the roots are a complex conjugate pair.

SIMULATION

A simulation of particle events was developed to test the three-observation and two-observation event reconstruction methods. The simulation parameters were chosen to roughly align with particle events observed about the asteroid Bennu by the OSIRIS-REx spacecraft [3], though they are not exactly the same. The asteroid was approximated as an oblate spheroid, with principal axes lengths $a = b > c$. The asteroid was modeled to rotate about its third principal axis (one with largest moment of inertia) with a constant angular velocity and was assumed to translate in the inertial frame with a constant velocity. The body parameters used in the simulation are summarized in Table 1.

Table 1. The particle body was roughly modelled on the physical parameters of Bennu.

Parameter	Value
Semi-Major Axis	300 m
Semi-Minor Axis	250 m
Angular Velocity	4.06×10^{-4} rad/s
Velocity (inertial frame)	$[0.4082, -0.8162, 0.4082]$ m/s

The simulation starts at time $t = 0$ with the body and spacecraft moving relative to each other. At the event time t_0, the particles are released from the body at a constant velocity. The particle velocities roughly corresponded to those measured by OSIRIS-REx [3]. The spacecraft then collects images at times t_i, where $i > 0$. Each image captures the direction to the observed particles at that instant in time. The full simulation parameters are outlined in Table 2.

Table 2. The simulation parameters were based off of observations from OSIRIS-REx, providing a physical grounding for the results.

Parameter	Value
Event time, t_0	150 sec
First observation, t_1	450 sec
Second observation, t_2	1650 sec
Third observation, t_3	2850 sec
Observation interval, δt	1200 sec
Observer velocity (inertial frame)	$[0.0254, 0.1270, 0.1524]$ m/s
Particle source (body frame)	$[198.8, 224.7, 0]$ m
Mean Particle Speed	14.37 cm/s
Min Particle Speed	11.4 cm/s
Max Particle Speed	18.4 cm/s

Three-Observation Case

In the three observation case, the spacecraft recorded n particle bearings at times t_1, t_2, and t_3. The bearings from the first two observations were used to estimate the direction to the particle origin, $\boldsymbol{\ell}_0$, as shown in Eq. (9). The cross-ratio for each particle was then calculated using Eq. (12). Because each particle follows a distinct path, n cross-ratios were determined, using the three observations of each particle and the estimated origin direction. Thereafter, the estimated event time, t_0, was calculated for each cross-ratio using Eq. (13). The t_0 estimates from all of the particles were then averaged to calculate a single estimate of the event time.

For a spacecraft with noiseless measurements of the particles' position and observation time, the three-observation method yielded perfect estimates of the particle event time. The time estimates were identical and perfect across particles, meaning the event time could be correctly determined from three observations of only a single particle.

A Monte Carlo simulation was performed to test the robustness of the cross-ratio method in the presence of measurement noise. The simulation introduced measurement errors in the particles' bearing directions and observation times. The simulation started by randomly generating trajectories from the particle source, following the same parameters outlined in Table 2. The particle directions were selected from a 45-degree ejecta cone oriented perpendicular to the asteroid's surface. At every observation time, the true particle bearings perturbed using the QUEST measurement model (QMM) [9, 10] with a standard deviation of 5 arcsec. Similarly, a normally distributed timing error was applied to each measurement with a standard deviation of 5 ms. The timing errors were the same for each particle particles, as they were assumed to be collected from a common image (and hence all have the same timetag error). After the errors were

introduced to the observation times and bearings, the event was reconstructed using the technique described in this manuscript.

The number of particles was varied from 5 to 100 to see the effect of this on reconstruction performance. A total of 10,000 trials were completed for each scenario. The t_0 estimate results with only bearing errors are shown in Fig. 3. The t_0 estimate results with both bearing and time measurement errors are shown in Fig. 4, and a comparison of Figs. 3 and 4 shows that the small 5 ms timing error has no meaningful effect on the quality of the reconstruction (as compared to the 5 arcsec bearing error). The errors in the estimated event direction with both timing and bearing errors are shown in Fig. 5. The errors in both event time and event direction decrease as more particles are observed. Moreover, these errors decrease as $1/sqrtn$ as one would expect from averaging.

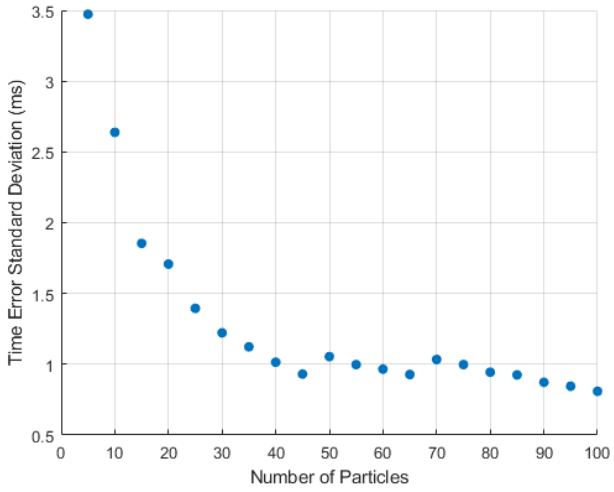

Figure 3. Error in estimated event time with only noise on bearing measurements (no time noise).

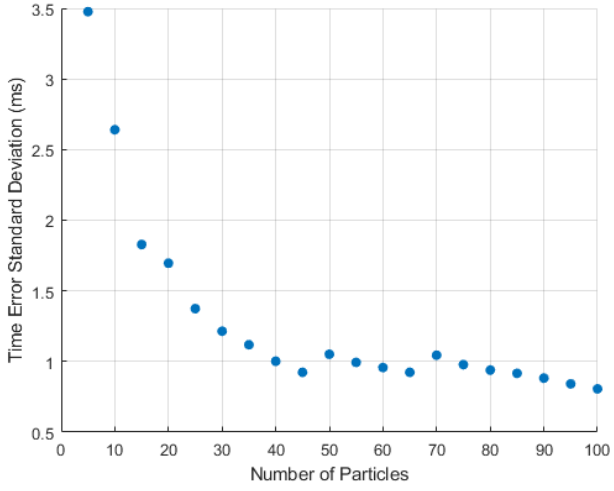

Figure 4. Error in estimated event time with both noisy bearing measurements and noisy time tags.

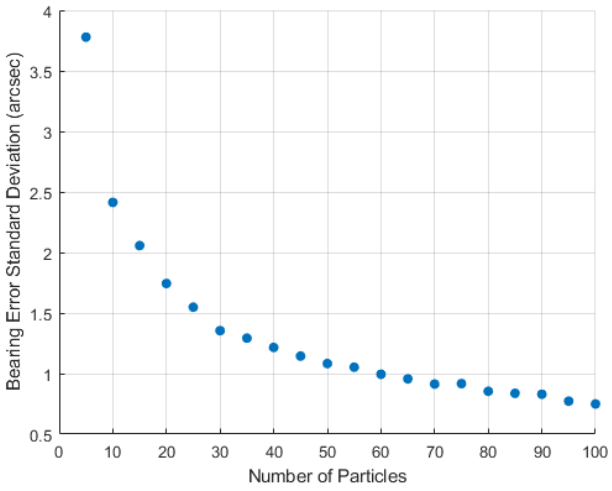

Figure 5. Error in estimated event direction with both noisy bearing measurements and noisy time tags.

Two-Observation Case

In the two-observation case, unambiguous estimation of event time is not possible. Despite this, a number of interesting results may still be produced. Therefore, consider the situation where particle observations are collected only at times t_1 and t_2. The bearings may be used to calculate the camera-relative direction to the event, $\boldsymbol{\ell}_0$, using Eq. (8). However, we cannot complete the reconstruction process since we cannot uniquely solve for t_0 with just two observation times.

While we cannot explicitly estimate t_0, we may bound it. First, we know that the event had to occur before the first observation at t_1—and so t_1 serves as a natural upper bound on the possible event times. Second, if images are taken at regular intervals (e.g, $\delta t = t_{i+1} - t_i$) and no particles were observed until the image at t_1, then a natural lower bound is $t_1 - \delta t$. Therefore, we restrict the possible event times to be on the interval $[t_1 - \delta t, t_1]$. We then perform a single-parameter sweep in t_0 across this range and complete the reconstruction with each possible event time.

Because the observed body is translating and rotating relative to the camera, the location where $\boldsymbol{\ell}_0$ changes with every different choice of t_0. In some cases within the range of possible times, the direction $\boldsymbol{\ell}_0$ may not intersect the observed body at all and these times may be discarded.

To see how this works in practice, consider a scenario with only four particles (still following the parameters outlined in Table 2). The particle directions of motion were chosen arbitrarily and the scenario is illustrated in Fig. 6. The observations of the particles at times $t_1 = 450$sec and $t_2 = 1650$sec were used to generate the estimates of the possible event locations. The event locations and their associated times are shown in Figs. 7 and 8, superimposed on the body and represented as a ground-track. The figures illustrate that the true particle source and its associated event time lie along the path found by the approach described here.

If we further restrict the cases to only allow scenarios where the body does not obstruct particle observations, then we find that not the entire path is not a physically valid solution. Using only the physically valid times greatly reduces the plausible times and locations of the event, as can be seen in Figs. 9 and 10. In this specific example, the valid range of event times is only 341 seconds, representing a large reduction over the original 1200 second search space. Though the two-particle method does not yield a unique estimate, it is an effective tool to reduce the search space of possible particle sources and times. In practice, the valid ground track could be interrogated in search of visible evidence of a past event.

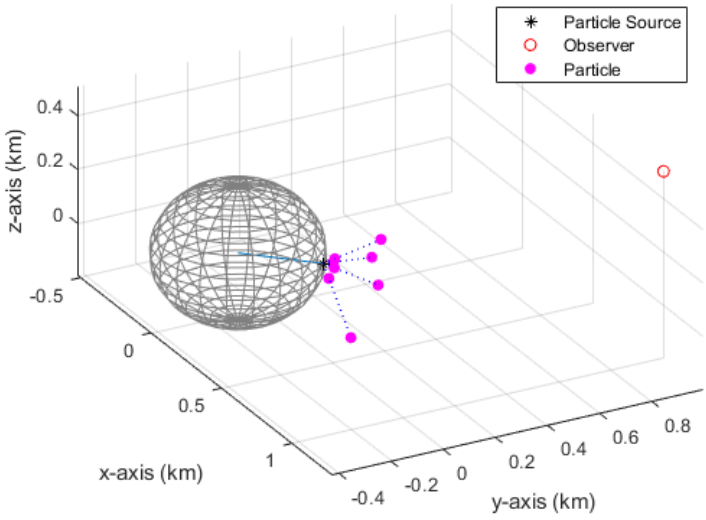

Figure 6. Illustration of the four-particle scenario used to demonstrate the two-observation event reconstruction scheme.

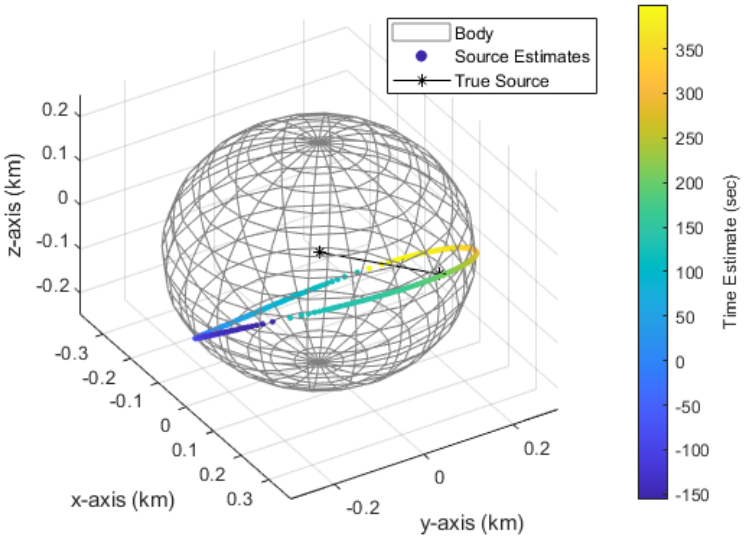

Figure 7. The 3D path of potential event locations is dependent on the assumed particle event time. This is due to the relative motion between the body and camera.

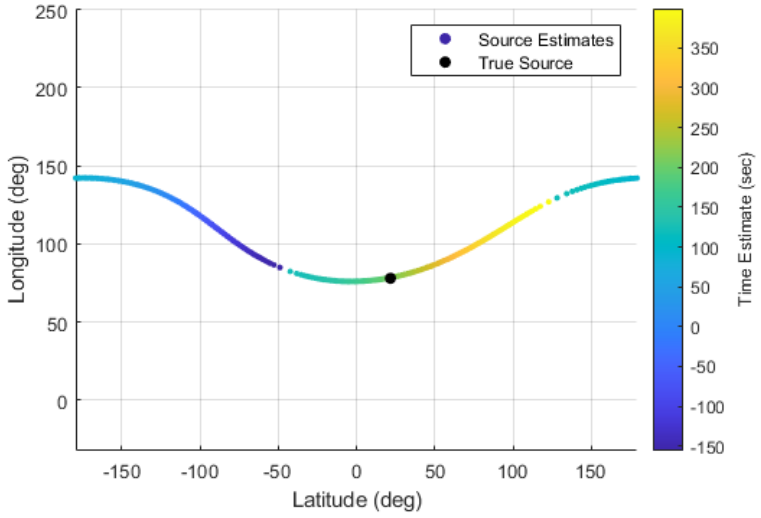

Figure 8. The ground track of potential event locations is dependent on the assumed particle event time.

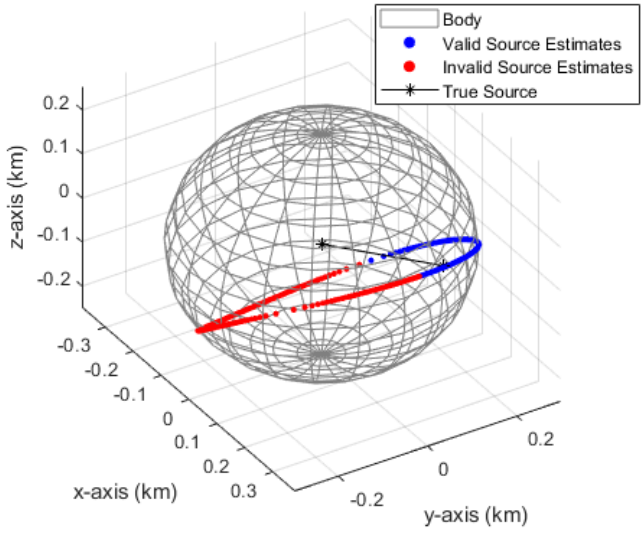

Figure 9. The relative geometry can be used to eliminate potential event times and locations. Only the blue portion of the 3D path is valid.

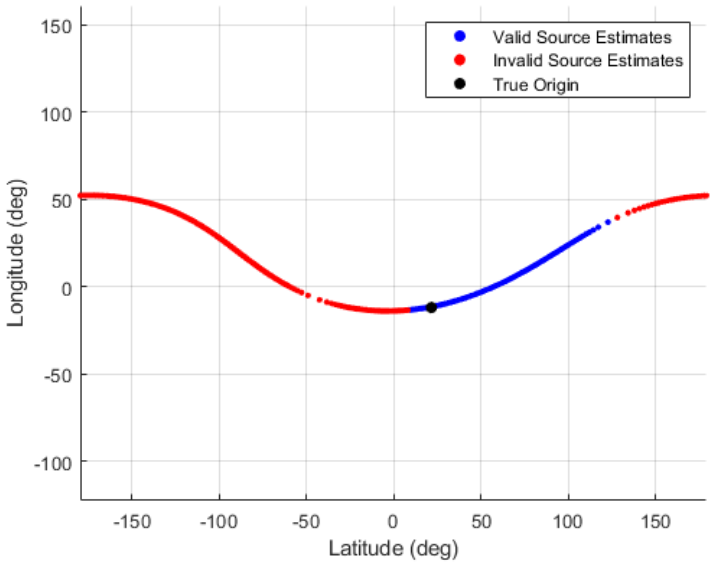

Figure 10. The plausible portion of the ground track of particle may be greatly reduced using the body's physical properties. Only the blue portion of the ground track is valid.

CONCLUSION

The observation of discrete particle ejection events on the asteroid Bennu motivates the development of techniques to efficiently reconstruct such events. Algebraic projective geometry is an effective tool for this task, as the cross-ratio of particle tracks may be used to simplify the analysis. Furthermore, analyzing the particles using the cross-ratio allows for greater insight into the event's geometry. In general, at least three observations of each particle (usually from three images, each containing all of the particles) is necessary to arrive at a unique solution for the event time and location. The three-observation case produces a perfect solution in the noise-free case and continues to function well in the presence of noise. For situations where only two observations (e.g., two images) are available, we may constraint the plausible locations on the body's surface where the event may have occurred.

REFERENCES

[1] D. Lauretta, S. Balram-Knutson, E. Beshore, W. Boynton, C. Drouet d'Aubigny, D. DellaGiustina, H. Enos, D. Golish, C. Hergenrother, E. Howell, C. Bennett, E. Morton, M. Nolan, B. Rizk, H. Roper, A. Bartels, B. Bos, J. Dworkin, D. Highsmith, D. Lorenz, L. Lim, R. Mink, M. Moreau, J. Nuth, D. Reuter, A. Simon, E. Bierhaus, B. Bryan, R. Ballouz, O. Barnouin, R. Binzel, W. Bottke, V. Hamilton, K. Walsh, S. Chesley, P. Christensen, B. Clark, H. Connolly, M. Crombie, M. Daly, J. Emery, T. McCoy, J. McMahon, D. Scheeres, S. Messenger, K. Nakamura-Messenger, K. Righter, and S. Sandford, "OSIRIS-REx: Sample Return from Asteroid (101955) Bennu," *Space Science Reviews*, Vol. 212, 2017, 10.1007/s11214-017-0405-1.

[2] D. S. Laurerra and et al., "Episodes of particle ejection from the surface of the active asteroid (101955) Bennu," *Science*, Vol. 366, No. 6470, 2019, 10.1126/science.aay3544.

[3] J. Y. Pelgrift, E. J. Lessac-Chenen, C. D. Adam, J. M. Leonard, D. S. Nelson, L. McCarthy, E. M. Sahr, A. Liounis, M. Moreau, B. J. Bos, C. W. Hergenrother, and D. S. Laurerra, "Reconstruction of Bennu Particle Events From Sparse Data," *Earth and Space Science*, Vol. 7, 2021, 10.1029/2019EA000938.

[4] J. G. Semple and G. T. Kneebone, *Algebraic Projective Geometry*. Oxford, UK: Oxford University Press, 1952.

[5] J. A. Christian, "A Tutorial on Horizon-Based Optical Navigation and Attitude Determination with Space Imaging Systems," *IEEE Access*, 2021, 10.1109/ACCESS.2021.3051914.

[6] J. A. Christian, H. Derksen, and R. Watkins, "Lunar Crater Identification in Digital Images," *The Journal of the Astonautical Sciences*, 2021.

[7] J. A. Christian and J. L. Crassidis, "Star Identification and Attitude Determination with Projective Cameras," *IEEE Access*, 2021, 10.1109/ACCESS.2021.3054836.

[8] S. Henry and J. A. Christian, "Absolute Triangulation Algorithms for Space Exploration," arXiv, https://arxiv.org/abs/2205.12197, 2022.

[9] M. D. Shuster and S. D. Oh, "Three-Axis Attitude Determination from Vector Observations," *Journal of Guidance and Control*, Vol. 4, No. 1, 1981, pp. 70–77, 10.2514/3.19717.

[10] M. D. Shuster, "Maximum Likelihood Estimation of Spacecraft Attitude," *The Journal of the Astronautical Sciences*, Vol. 37, No. 1, 1989, pp. 79–88.